

Dedicated to Prof. Dorin N. Poenaru's  
70th Anniversary

## BINARY AND TERNARY SPONTANEOUS FISSION IN $^{252}\text{Cf}$

A.V. RAMAYYA, J.H. HAMILTON, J.K. HWANG

Department of Physics, Vanderbilt University, Nashville, TN 37235, USA

(Received January 2, 2007)

*Abstract.* Triple coincidence data from the fission of  $^{252}\text{Cf}$  were used to deduce the intensity of the proposed second mode in barium channels by using the  $\gamma - \gamma - \gamma$  coincidence relations and Gammasphere. An upper limit of 1.25% was found for the relative intensity of the second mode in the Ba-Mo case. Yields for cold ternary and cold binary fission were extracted from intensities of  $\gamma$ -ray transitions originating from the de-excitation of primary and secondary fragments. The relative  $^4\text{He}$  and  $^5\text{He}$  ternary fission yields were determined from a careful analysis of the energy distribution of  $\alpha$  spectra from a new measurement with a  $^{252}\text{Cf}$  source and from published data on  $^{252}\text{Cf}$  and  $^{235}\text{U}(\text{n},\text{f})$ . The kinetic energies of the  $^5\text{He}$  and  $^4\text{He}$  ternary particles were found to be approximately 11 and 16 MeV, respectively.  $^5\text{He}$  particles contribute 10-20% to the total alpha yield with the remainder originating from ternary fission accompanied by the emission of  $^4\text{He}$ . A number of correlated pairs are identified in ternary fission with  $^{10}\text{Be}$  as the LCP. We observed only cold, 0n  $^{10}\text{Be}$  and little, if any, hot, xn  $^{10}\text{Be}$  channel.

*Key words:* binary and ternary spontaneous fission, triple and double gamma coincidences, gammasphere.

### 1. INTRODUCTION

The last decade has seen great advances in the study of prompt  $\gamma$ -rays accompanied spontaneous fission. With the development of large Ge detector arrays, such as Gammasphere and Eurogam which offer high degree of sensitivity and selectivity, quantitative determination of rare processes such as cold binary and cold ternary fission processes, have become feasible. The so-called “cold-fission” processes are the ones where no neutrons are emitted. In these types of experiments, one measures the coincidence relationships among the

$\gamma$ -rays emitted by the two fission fragments. From such measurements [1], one can extract the yields for many types of rare processes. Also, it is possible to study the weak intensities of the hot mode in the binary fission by using the triple  $\gamma$  coincidences and Gammasphere. In the present review paper, we present the topics of the binary spontaneous fission (SF) and  $\alpha$  and  $^{10}\text{Be}$  ternary spontaneous fission.

## 2. SECOND MODE IN THE BINARY FISSION

Observations of prompt  $\gamma$ -rays produced in the spontaneous fission of  $^{252}\text{Cf}$  have shown evidence for a second fission mode in the Ba-Mo channel. The evidence for this mode is observed as a higher relative intensity for the 7–10 neutron channels [2–4]. A later analysis [5, 6] shows a much smaller second mode, but did find an “irregularity” around the eight-neutron channel. In recent years, more complete data on the levels and relative intensities of transitions in barium and molybdenum isotopes have become available. Because fission spectra are often complex and the events of interest are rare compared with other channels, this type of analysis is difficult and prone to errors caused by random coincidences and background. Therefore an improved method which avoids many of these complexities was developed in order to determine the relative intensity of the second mode in both the binary and ternary cases involving barium.

The data for this analysis come from experiments with the Gammasphere detector array when located at Lawrence Berkeley National Laboratory. A  $62\mu\text{Ci}$  source was placed between two iron foils in order to stop fission fragments. This arrangement was then put in a 7.62 cm polyethylene ball and placed in Gammasphere. A total of  $5.7 \times 10^{11}$   $\gamma - \gamma - \gamma$  events were recorded. A coincidence cube was then constructed using the Radware software package [7].

The number of prompt neutrons emitted in a binary fission event can be determined by finding the mass number of the fragments produced in the event. For example, if the fission fragments of  $^{252}\text{Cf}$  are determined by some method to be  $^{144}\text{Ba}$  and  $^{103}\text{Mo}$ , then five neutrons must have been emitted. The relative intensities of a particular neutron channel can be found from triple coincidence data by double gating on a pair of transitions in the heavy fragment, then measuring the intensity of its partners. This must be done for each isotope of the heavy partner. The yield as a function of neutrons emitted can then be determined by summing the contributions of all possible pairs. More details can be found in Ref. [8].

Table 1

Relative Yield Matrix for the Ba-Mo charge split

Ba\Mo	102	103	104	105
138				0.43(25)
139			0.41(8)	0.36(12)
140		0.4(1)	0.19(12)	2.9(9)
141		1.2(9)	1.8(8)	13.0(7)
142	0.007(3)	6(1)	27.0(7)	45.9(9)
143	4(1)	18.6(8)	59.4(9)	93(3)
144	10.0(3)	51(1)	102(4)	99(2)
145	21(1)	53(2)	79(2)	46(2)
146	16.7(7)	30.6(6)	39(3)	11.0(2)
147	4.3(2)	14.5(4)	5.1(4)	2.1(2)
148	2.1(2)	1.8(2)	0.5(2)	
Ba\Mo	106	107	108	109
138			0.78(36)	
139	2.3(2)	2.7(6)	4.8(8)	2.5(1)
140	11.8(6)	11(1)	22(5)	2.5(2)
141	37(1)	26(3)	39(3)	3.2(3)
142	92(2)	41(2)	51(33)	5.5(2)
143	111(2)	32(3)	59(9)	2.8(8)
144	71.7(2)	10(1)		
145	21.9(9)			
146	4.5(2)			

The Xe-Ru binary channel was the first to be analyzed. The resulting neutron distribution is fit well by a single Gaussian; there is no second mode. However, in the Ba-Mo case, there is still a higher than expected yield for 9-neutron channel, as shown in Fig. 1. This could be evidence for a second mode, but it is difficult to interpret this result in the usual way since this distribution is not fit well by a double Gaussian. An upper limit for the intensity of the second mode in this case was determined by taking the  $2\sigma$  upper limits for the 8 and 9 neutron channels and fitting this distribution to a double Gaussian with the requirement that the first mode be centered around 3 neutrons and the second mode be centered at  $>6$  neutrons. If there is indeed a second mode in the Ba-Mo split, this analysis suggests that the intensity is below 1.25% of the primary mode.

### 3. COLD BINARY SPONTANEOUS FISSION

Since the neutronless binary events are much smaller than those with neutrons emitted, double gating techniques have been employed to extract

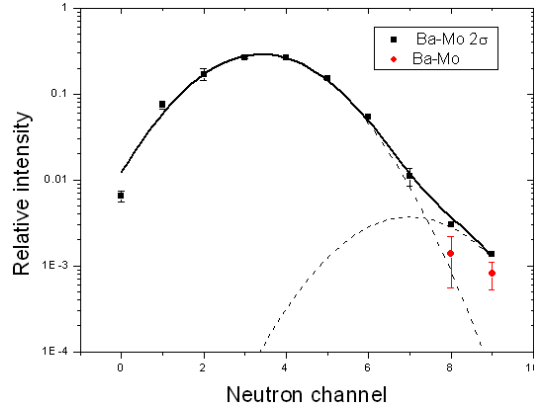


Fig. 1 – Upper limit for the intensity of the 2<sup>nd</sup> mode in the Ba-Mo split.

the yields for the cold binary fission. No direct measurements of yields of correlated pairs in cold binary fission have been made prior to our work. Earlier we reported the first results for the correlated pairs in cold binary fission in  $^{252}\text{Cf}$  [3, 9, 10] and  $^{242}\text{Pu}$  [11]. Subsequently we extracted more detailed yields of cold binary fission from Gammasphere data with 72 detectors [12].

Table 2

Average cold binary fission yields from gates on two light fragment and two heavy fragment transitions [12]

	$A_L / A_H$	$Y_{exp}$	$Y_{the}$	$Y_{the}^{(ren)}$
Zr/Ce	100/152	0.010(2)	0.38	0.004
	102/150	0.020(4)	2.82	0.033
	103/149	0.030(6)	4.21	0.049
	104/148	0.010(2)	1.03	0.012
Mo/Ba	104/148	0.010(2)	0.47	0.005
	105/147	0.040(8)	5.39	0.063
	106/146	0.040(8)	0.61	0.007
	107/145	0.070(14)	3.07	0.036
	108/144	0.030(6)	7.45	0.087
Tc/Cs	109/143	0.090(18)	11.03	0.128
Ru/Xe	110/142	0.060(12)	3.78	0.044
	111/141	0.10(2)	7.12	0.083
	112/140	0.020(4)	0.59	0.007
	114/138	0.020(4)	1.17	0.014
Pd/Te	116/136	0.050(20)	2.35	0.027

By determining the intensities of  $\gamma$  transitions in both fragments and knowing the branching ratios between different transitions, the relative binary

yields [12] were extracted again where the total yield was normalized to Wahl's table [13]. Presently, many of the spectra of the odd- $Z$  nuclei are not known, so that one could not determine experimentally most odd- $Z$  isotopic yields. The cold binary fission yields are shown in Table 2 along with the theoretical values predicted by Sandulescu *et al.* [14]. In Table 2, the first report of the cold binary fission of an odd- $Z$  – odd- $Z$  fragmentation is shown for the Tc and Cs pair.

Based on a cluster model similar to the one-body model used for the description of cluster radioactivity [15] in which the barrier between fragments can be calculated quite accurately due to the fact that the touching configurations are situated inside of the barriers, Sandulescu *et al.* [9, 11] predicted the relative isotopic yields for the spontaneous cold (neutronless) binary, and  $\alpha$ -ternary [15] fragmentations of  $^{252}\text{Cf}$ , taken as ratios of the penetrability of a given fragmentation over the sum of penetrabilities of all possible (neutronless) fragmentations.

In the case of cold ternary fission, Sandulescu *et al.* [9, 11] considered that close to the scission configuration a few of the nucleons form a short neck. At a given value of the neck radius a double scission takes place, a third light fragment is formed between the two heavier ones and from this point starts the ternary fission barrier corresponding to a given mass and charge splitting [14]. The trends, e.g. variations with  $A$  and  $Z$ , of the theoretically calculated yields are in good agreement with the experimental yields. Of particular note, for even  $Z$  the odd  $A$ -odd  $A$  pairs are predicted to be larger than the even  $A$  – even  $A$  pairs and this is observed in every case. Moreover the largest theoretical yield predicted is for the odd  $Z$  – odd  $Z$   $^{109}\text{Tc}$  –  $^{143}\text{Cs}$  and this is true within the experimental error. Overall these results generally are in remarkable agreement.

#### 4. COLD $\alpha$ TERNARY SPONTANEOUS FISSION

Hot ternary fission has been known for a long time, with the third particle generally being an  $\alpha$  particle. However, cold ternary fission had not been directly observed prior to our work [16]. In the case of cold (neutronless) alpha ternary fission of  $^{252}\text{Cf}$ , one looks at the correlation between two even- $Z$  fragments with the sum of charges  $Z = 96$  and sum of masses  $A = 248$ . For example,  $^{146}_{56}\text{Ba}$  and  $^{102}_{40}\text{Zr}$  are the partners when a ternary  $\alpha$ -particle is involved. More experimental details can be found in Ref. [16].

In Table 3, the cold neutronless alpha ternary fission yields observed in the spontaneous fission of  $^{252}\text{Cf}$  are presented. The highest experimental yields were found for the Zr + Ba isotopes. Significant yields also were observed for

the Mo + Xe and Sr + Ce ternary fragmentations. The average values of the  $\alpha$  ternary fission yields obtained by double-gating on the heavy fragments or light fragments are listed in Table 3. The theoretical values calculated by Sandulescu *et al.* [17] are shown in columns 3 and 6 of Table 3. Since a different normalization is used for the theoretical calculations, the total theoretical yield is normalized to the total experimental yield, and the reported values are the renormalized relative theoretical yields. In general, there is good agreement between the relative theoretical and experimental yields.

Table 3

The alpha ternary isotopic yields  $Y_{exp}$  obtained per 100 fission events [16]

$\alpha$ Partner nuclei	$Y_{exp}$ (%)	$Y_{the}^{ren}$	$\alpha$ Partner nuclei	$Y_{exp}$ (%)	$Y_{the}^{ren}$
$^{92}_{36}\text{Kr}-^{156}_{60}\text{Nd}$	0.002(1)	0.002	$^{96}_{38}\text{Sr}-^{152}_{58}\text{Ce}$	0.008(3)	0.010
$^{98}_{38}\text{Sr}-^{150}_{58}\text{Ce}$	0.014(6)	0.017	$^{99}_{38}\text{Sr}-^{149}_{58}\text{Ce}$	0.018(9)	0.016
$^{100}_{38}\text{Sr}-^{148}_{58}\text{Ce}$	0.021(10)	0.027	$^{101}_{38}\text{Sr}-^{147}_{58}\text{Ce}$	0.014(11)	0.010
$^{100}_{40}\text{Zr}-^{148}_{56}\text{Ba}$	0.038(12)	0.017	$^{101}_{40}\text{Zr}-^{147}_{56}\text{Ba}$	0.082(10)	0.058
$^{102}_{40}\text{Zr}-^{146}_{56}\text{Ba}$	0.009(4)	0.017	$^{103}_{40}\text{Zr}-^{145}_{56}\text{Ba}$	0.084(29)	0.050
$^{104}_{40}\text{Zr}-^{144}_{56}\text{Ba}$	0.017(8)	0.016	$^{106}_{42}\text{Mo}-^{142}_{54}\text{Xe}$	0.018(7)	0.031
$^{107}_{42}\text{Mo}-^{141}_{54}\text{Xe}$	0.030(14)	0.017	$^{108}_{42}\text{Mo}-^{140}_{54}\text{Xe}$	0.007(3)	0.014
$^{112}_{44}\text{Ru}-^{136}_{52}\text{Te}$	0.011(6)	0.028	$^{116}_{46}\text{Pd}-^{132}_{50}\text{Sn}$	0.006(3)	0.048

A few of the cold  $\alpha$ -ternary fragmentations presented in Table 3 involve odd-odd splittings. One observes that their corresponding experimental yields are higher than the yields for the even-even neighbours, as found in the theoretical calculations also. The increased yields in these cases may be because of the differences in level densities near the ground states in odd-odd and the even-even nuclei. The enhanced experimental yields for the cold  $\alpha$ -ternary fission in which heavier partners are Ba isotopes could be attributed to the static octupole deformation observed in this region, since octupole shapes at the scission configuration could significantly lower the Coulomb barrier and increase the penetrability between the final fragments. These are the first identification and determination of yields of the particular correlated pairs associated with cold  $\alpha$  ternary fission.

## 5. LIGHT CHARGED PARTICLE TERNARY FISSION

Another experiment was performed incorporating light charged particle (LCP) detectors to detect ternary particles in coincidence with  $\gamma$  rays in Gammasphere. The energy spectra of LCPs emitted in the spontaneous fission of

$^{252}\text{Cf}$  were measured by using two  $\Delta E - E$  Si detector telescopes installed at the center of the Gammasphere array. With the position resolution of the strip detector (4 mm wide strips and 1 mm resolution along each strip), the  $\Delta E - E$  telescopes provided unambiguous  $Z$  and  $A$  identification for all the LCPs of interest. The  $\gamma$ -ray spectrum in coincidence with ternary  $\alpha$ -particles is shown in Fig. 2. In this spectrum, one can easily see the  $\gamma$ -transitions for

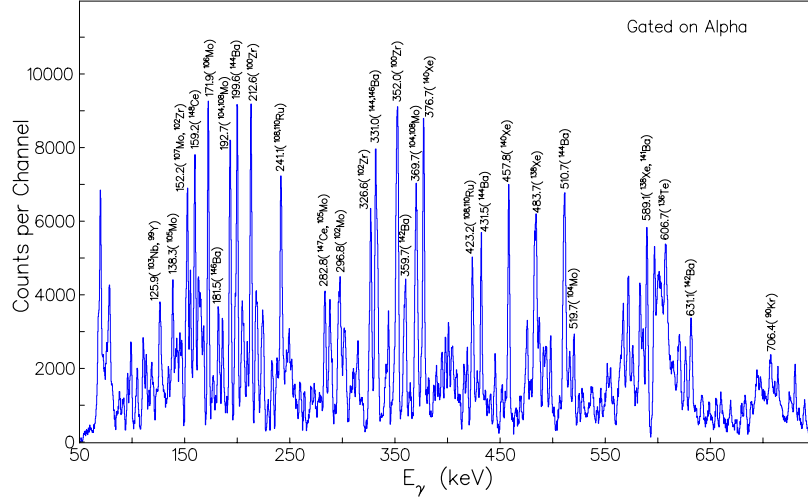


Fig. 2 –  $\gamma$ -ray spectrum in coincidence with  $\alpha$ -particles.

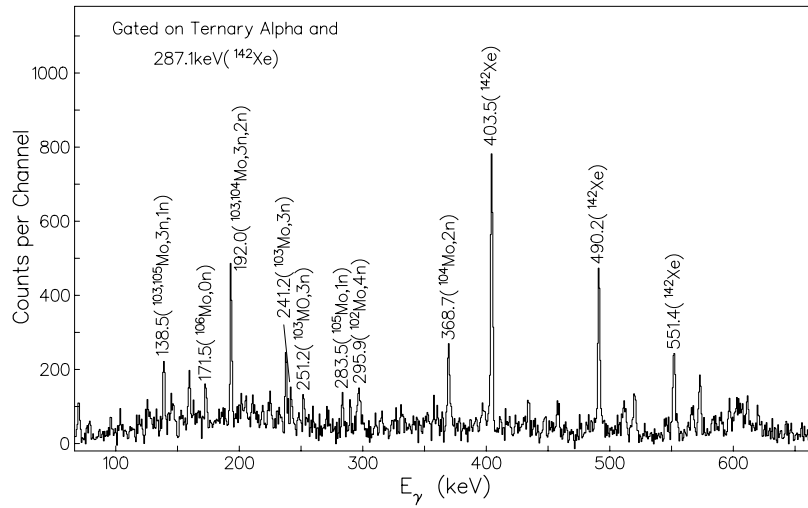


Fig. 3 – Coincident spectrum gated on  $\alpha$  and 287.1 keV transition in  $^{142}\text{Xe}$ .

various partner nuclei where a ternary  $\alpha$ -particle is emitted. For example, Xe

and Mo isotopes are partners where  $\alpha$  and xn are emitted. Now, imposing an additional condition that the  $\alpha$ -gated  $\gamma$ -spectrum should be also in coincidence with the  $2^+ \rightarrow 0^+$  transition in  $^{142}\text{Xe}$ , one gets a very clean spectrum as shown in Fig. 3. From the analysis of the  $\gamma$ -ray intensities in these types of spectra, one can calculate the yield distributions. The yield distributions both for binary and ternary  $\alpha$ -channel from 0 to 6n emission are shown Fig. 4 for two particular channels. These are the first relative 0-6n yields for any ternary

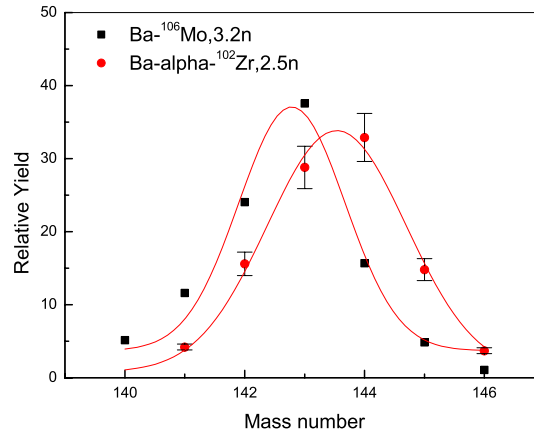


Fig. 4 – Yield spectrum for  $\alpha$ .

$\alpha$  SF. Note the peak of the neutron emission yields for Ba- $\alpha$ - $^{102}\text{Zr}$  is shifted up by about half an AMU from the Ba- $^{106}\text{Mo}$  binary yield and so the average neutron emission in this  $\alpha$  ternary SF channel is shifted down by about 0.4n. About 5-20 % of the  $\alpha$  yield is from  $^5\text{He}$  ternary fission in  $^{252}\text{Cf}$  SF.

## 6. $^5\text{He}$ TERNARY FISSION YIELDS [18] OF $^{252}\text{Cf}$ AND $^{235}\text{U}$

In the case of  $^{252}\text{Cf}$ , the relative yields of  $^4\text{He}$ ,  $^6\text{He}$  and  $^8\text{He}$  have been measured to be  $10^4$ , 393(60), and 25(5), respectively, with an absolute ternary  $^4\text{He}$  yield of  $3.82 \times 10^{-3}$  [19]. The contribution of  $^5\text{He}$  to the ternary helium fission yield is difficult to determine because of its break-up into the  $\alpha + n$  channel with a half-life of  $8 \times 10^{-22}$ . The  $Q$  value and neutron energy associated with this process are 0.957 MeV and 4.0(3) MeV, respectively [20], e.g.  $\langle E_{^5\text{He}} \rangle = \langle E_{\alpha} \rangle + 3\text{MeV}$ . The presence of  $^5\text{He}$  in the fission of  $^{252}\text{Cf}$  was originally demonstrated by Cheifetz *et al.* [21], who measured the correlation between neutrons and  $\alpha$  particles at  $0^\circ$  and  $180^\circ$ , and reported that approximately 11(2)% of the ternary  $\alpha$  particles result from  $^5\text{He}$  break-up. The

average  $^5\text{He}$  kinetic energy was measured to be 15.4 MeV, i.e. the associated  $\alpha$  energy is 12.4(9) MeV [21]. The latter value should be contrasted with the *average*  $\alpha$  energy of 15.7 MeV reported in Ref. [19]. The results of Refs. [20–23] leave a number of open questions. The mean  $^5\text{He}$  energy of  $\sim 6$  MeV extracted from the low-energy tail of the  $\alpha$  spectra [22,23] differs significantly from the only direct measurement of 12.4 MeV [21]. Furthermore, the  $^5\text{He}$  yield extracted from this tail, 15.5 % [22, 23], is barely consistent with the yield of 11 % reported by Cheifetz *et al.* [21]. Additional uncertainties regarding the experimental situation come from the fact that the role of the neutron multiplicity was not considered in Ref. [21]. This multiplicity was determined later by Han Hongyin *et al.* [24]. Thus, it appeared worthwhile to revisit the issue. Hereafter, we present the results of a new analysis of  $\alpha$  spectra from ternary fission. Data from a new measurement with a  $^{252}\text{Cf}$  source as well as published data on  $^{252}\text{Cf}$  and  $^{235}\text{U}(\text{n},\text{f})$  have been analyzed. A consistent picture of the  $^5\text{He}$  ternary fission yield appears to emerge. An approach to the fitting procedure was then employed with the only requirement that the widths of the two Gaussian distributions be the same, hereby fulfilling the requirement derived from Ref. [22]. This approach neglects the fact that the break-up of  $^5\text{He}$  contributes a small, additional spread in momentum to the distribution imparted by the ternary fission process. The results given in Table 3 are presented under the assumption that  $^4\text{He}$  ternary fission dominates the alpha particle spectra, i.e. that  $^5\text{He}$  is associated with the component with the smaller intensity. The results of the fit are also displayed in the top part of Fig. 5. The energies associated with the two particles are now quite different, even though the centroid of the low-energy Gaussian is determined with less than desirable accuracy. This is due to the low-energy cut-off of the present  $\alpha$  spectra. This cut-off also impacts severely the accuracy with which the intensity of the two components can be determined. In other words, the low-energy cut-off of the present  $\alpha$  spectra makes the errors large in the yields and energies as shown in Table 4. These findings prompted us to then concentrate on the data of Loveland [23] and the results of a fit (with the same constraints) of the spectrum measured by this author are presented in Table 4 and the middle part of Fig. 5. Within the errors, the results of the two data sets are in satisfactory agreement. Furthermore, the effect of the low-energy cut-off in the new data was examined by arbitrarily truncating the data by Loveland [22]. It was found that the changes in the values of the fitting parameters remained within errors for cut-off energies varying from  $\sim 1$  to 9.5 MeV; i.e., the values presented in Table 4 are quite stable and reliable.

Thus, this analysis indicates that the average energies of the alpha particles associated with  $^4\text{He}$  and  $^5\text{He}$  differ by 3–6 MeV and that at least 80 % of the total alpha yield is associated with  $^4\text{He}$  originating from ternary fission.

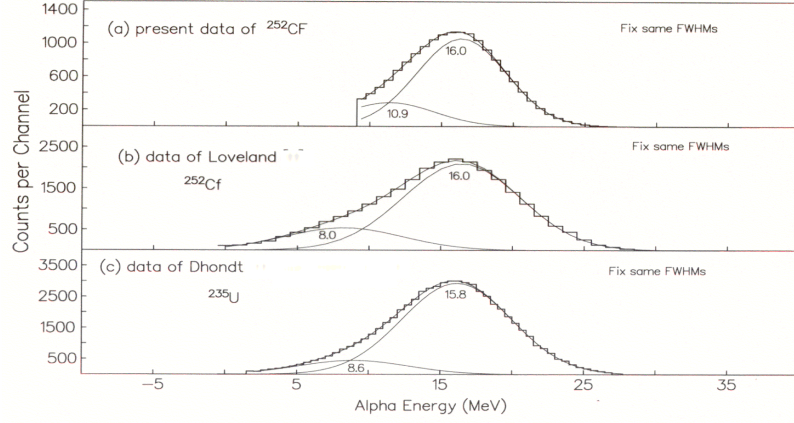


Fig. 5 – Two Gaussian fits with the only condition of the same FWHMs for two Gaussians: (a) this spectrum is from our work [18]; (b) and (c) from data of Loveland [23] and from data of D’hondt *et al.* [25, 26], respectively.

Table 4

Relative yield ratios extracted for the ternary  ${}^4\text{He}$  and  ${}^5\text{He}$  particles of  ${}^{252}\text{Cf}$  from our work [18] (first and second rows) and Ref. [23] (third and fourth rows) for  ${}^{252}\text{Cf}$ , and from Ref. [25, 26] (last rows) for  ${}^{235}\text{U}(n,f)$ .

$$\langle E_{5\text{He}} \rangle = \langle E_{\alpha} \rangle - Q + \langle E_n \rangle = \langle E_{\alpha} \rangle + 3 \text{ (MeV)} [20]$$

		$\langle E \rangle$ MeV	FWHM MeV	Relative yields	$\chi^2/\text{d.o.f}$
${}^{252}\text{Cf}$	${}^4\text{He}$	$16.0^{+1.0}_{-0.5}$	$7.4^{+0.4}_{-0.8}$	$79.6^{+12.0}_{-24.4}$	0.068
	${}^5\text{He}$	$13.9^{+1.1}_{-4.3}$	$7.4^{+0.4}_{-0.8}$	$20.4^{+21.9}_{-2.9}$	
${}^{252}\text{Cf}$	${}^4\text{He}$	$16.0^{+0.3}_{-0.3}$	$9.7^{+0.3}_{-0.3}$	$78.9^{+4.9}_{-4.1}$	0.91
	${}^5\text{He}$	$11.0^{+0.5}_{-1.0}$	$9.7^{+0.3}_{-0.3}$	$21.1^{+3.9}_{-4.5}$	
${}^{235}\text{U}$	${}^4\text{He}$	$15.8^{+0.4}_{-0.3}$	$9.1^{+0.4}_{-0.3}$	$87.7^{+4.7}_{-5.4}$	0.56
	${}^5\text{He}$	$11.6^{+0.9}_{-1.4}$	$9.1^{+0.4}_{-0.3}$	$12.3^{+5.2}_{-4.5}$	

Finally, a similar analysis of the  ${}^{235}\text{U}(n,f)$  ternary fission data of Refs. [25] and [26] was also carried out. The results form the last entries to Table 3. As can be seen the results are similar to those obtained for  ${}^{252}\text{Cf}$  and a satisfactory understanding of the data appears to emerge. The agreement between the various data sets can be regarded as satisfactory, considering that the comparisons cover data obtained with independent instruments under different experimental conditions. A consistent description of the present  ${}^{252}\text{Cf}$  data

as well as of the data of Ref. [23] for  $^{252}\text{Cf}$  and of Refs. [25,26] for  $^{235}\text{U}(\text{n},\text{f})$  was achieved. In all cases the energy of  $^5\text{He}$  is determined to be around 11 MeV while the corresponding energy for  $^4\text{He}$  is 16 MeV. 80–90 % of the total yield can be assigned the ternary fission accompanied by a  $^4\text{He}$  particle. The remaining 10–20 % of the alpha yield is then assigned the break-up of  $^5\text{He}$ .

## 7. COLD $^{10}\text{Be}$ TERNARY SPONTANEOUS FISSION [12]

Ternary fission is very rare process that occurs roughly only once in every 500 spontaneous fissions (SF) dominated by  $\alpha$  ternary fission. Roughly, the  $^{10}\text{Be}$  particles are emitted once per  $10^5$  spontaneous fissions. The maximum yield in the binary spontaneous fission is located around 3 to 4 neutrons. We know that the  $\alpha$  ternary fission is, mostly, accompanied by  $\approx 2$  to 3 neutrons. In neutronless ternary spontaneous fission (SF), the two larger fragments have very low excitation energy and high kinetic energies. Experimentally it is not easy to identify the  $\gamma$  transitions of the cold or hot  $^{10}\text{Be}$  ternary SF pair because it is very rare process. The first case of neutronless  $^{10}\text{Be}$  ternary spontaneous fission (SF) in  $^{252}\text{Cf}$  was reported from  $\gamma - \gamma - \gamma$  coincidence spectrum where the pairs are  $^{96}\text{Sr}$  and  $^{146}\text{Ba}$  without neutrons emitted [27]. In our LCP- $\gamma - \gamma$  data, the cover foils allowed only the high energy tail of the  $^{10}\text{Be}$  energy spectrum to be observed in the particle detector and their partners established from the cube data.

In our work, the neutronless (cold)  $^{10}\text{Be}$  ternary spontaneous fission (SF) pairs of  $^{252}\text{Cf}$  are identified for two other fragment pairs of  $^{104}\text{Zr}$ - $^{138}\text{Xe}$  and  $^{106}\text{Mo}$ - $^{136}\text{Te}$  from the analysis of the  $\gamma - \gamma$  matrix gated by the  $^{10}\text{Be}$  particles as shown in Fig. 6. Also, several isotopes related to the  $^{10}\text{Be}$  ternary SF are

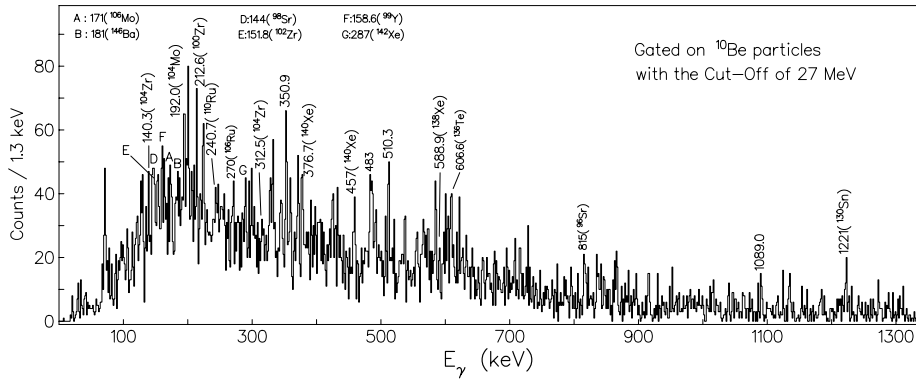


Fig. 6 –  $\gamma$ -ray spectrum in coincidence with  $^{10}\text{Be}$ .

observed. From the  $\Delta E$ - $E$  plot, the  $^{10}\text{Be}$  charged particles are selected as a gate

to make the  $\gamma-\gamma$  matrix. Also, we did not subtract the background spectrum from the full projection of the  $\gamma-\gamma$  matrix because of poor statistics. The high efficiency of Gammasphere enables coincidence relationships to be established even with the low statistics data associated with a small  $^{10}\text{Be}$  ternary SF yield. The identification of the gamma-transitions belonging to other partner fragments is not clear in this experiment. From the  $\gamma-\gamma-\gamma$  cube we could clearly establish coincidence for  $^{100}\text{Zr}-^{142}\text{Xe}$  and  $^{102}\text{Zr}-^{140}\text{Xe}$ . Also, by double gating on the 376.7 and 457.3  $\gamma$ -rays in  $^{140}\text{Xe}$ , we can see clearly the zero neutron channel  $^{102}\text{Zr}$  and probably the  $^{100}\text{Zr}$  2n channel which is weaker by a factor of 5-10 if present. The identification of several isotopes related with the  $^{10}\text{Be}$  emission is made by the observation of two or three transitions in coincidence belonging to each isotope and from the  $\gamma-\gamma-\gamma$  cube. All isotopes and the related  $\gamma$  transitions identified in the present work are tabulated in Table 5.

Table 5

Fragments identified from the coincidence relationship between  $\gamma$ -rays and  $^{10}\text{Be}$  ternary particle [12]. \* : identified in  $\gamma-\gamma-\gamma$  data and \*\* : LCP- $\gamma-\gamma$  data

Identified Isotopes ( $\beta_2$ [28, 29])	Observed $\gamma$ rays (keV) in the left column isotopes	Partner isotopes ( $\beta_2$ [28, 29])
$^{100}_{40}\text{Zr}$ (0.321 )	212.6, 352.0, 497.0	$^{142}_{54}\text{Xe}$ (0.145)*
$^{102}_{40}\text{Zr}$ (0.421 )	151.8, 326.2	$^{140}_{54}\text{Xe}$ (0.1136 )*
$^{104}_{40}\text{Zr}$ (0.381 )	140.3, 312.5	$^{138}_{54}\text{Xe}$ (0.0309 )**
$^{104}_{42}\text{Mo}$ (0.325 )	192.0, 368.5	$^{138}_{52}\text{Te}$ (0.000 )
(or $^{108}_{42}\text{Mo}$ )		(or $^{134}_{52}\text{Te}$ )
$^{106}_{42}\text{Mo}$ (0.353 )	171.6 with 606.6 ( $^{136}\text{Te}$ )	$^{136}_{52}\text{Te}$ (0.000 )**
$^{110}_{44}\text{Ru}$ (0.303 )	240.7, 422.2	$^{132}_{50}\text{Sn}$ (0.000 )
(or $^{108}_{44}\text{Ru}$ )		(or $^{134}_{50}\text{Sn}$ )
$^{136}_{52}\text{Te}$ (0.000 )	606.6, 424.0 with 171.6 ( $^{106}\text{Mo}$ )	$^{106}_{42}\text{Mo}$ (0.353)**
$^{138}_{54}\text{Xe}$ (0.0309 )	588.9, 483.8, 482.1	$^{104}_{40}\text{Zr}$ (0.381 )**
$^{140}_{54}\text{Xe}$ (0.1136 )	376.7, 457.4, 582.5	$^{102}_{40}\text{Zr}$ (0.421 )*

In Table 5, partner fragments pertaining to the cold (neutronless) channel are shown some of which are confirmed as noted. Quadrupole deformations for each isotopes are taken from Refs. [28, 29]. From these examples, we can see that the statistics of the coincident spectrum with a single gate on the lowest gamma transition does not depend on the statistics of the gated peak because of complexity of the gamma-ray multiplicity and the enhanced population of the lowlying levels in the  $^{10}\text{Be}$  SF.

The hot fission mode can excite the fragments up to higher level energies than the cold fission. The present results indicate that the cold (neutronless) process is dominant in the ternary SF accompanying a heavy third particle such as  $^{10}\text{Be}$  with high kinetic energy. In our work, we are gating only on the high kinetic energy part of the  $^{10}\text{Be}$  particles.

The  $^{104}\text{Zr}$  isotope is highly deformed with a  $\beta_2$  value of around 0.4 [7, 29] and the  $^{138}\text{Xe}$  nucleus is very spherical. Therefore, the  $^{10}\text{Be}$  particle seems to be emitted from the breaking of  $^{148}\text{Ce} = ^{138}\text{Xe} + ^{10}\text{Be}$  at scission which would enhance the  $^{10}\text{Be}$  kinetic energy. Increased deformation at the scission point increases excitation energy for the third ternary particle and two heavy fragments. Therefore the possibility of observing the excited levels in both the fragments increases when both of them are deformed at scission point such as  $^{104}\text{Zr}(\text{deformed}) - ^{148}\text{Ce}(^{138}\text{Xe} + ^{10}\text{Be})(\text{deformed})$ . Actually, the neutronless binary fission yield for  $^{148}\text{Ce} - ^{104}\text{Zr}$  pair is as high as 0.05(3) per 100 SF of  $^{252}\text{Cf}$  [30]. This case is very similar to the one we reported earlier for the pair  $^{96}\text{Sr}$  (spherical shape) and  $^{146}\text{Ba}$  (deformed shape) [27].

In the  $\alpha$  ternary fission we see the cold, zero, neutron fission but 2n and 3n channels are much stronger. However, for the cold  $^{10}\text{Be}$  ternary SF pairs identified from the  $\gamma - \gamma$  matrix gated on  $^{10}\text{Be}$  charged particles and the cube data, we find the zero neutron channel clearly much stronger than 1n and 2n. This is a very unique discovery in the study of the cold (zero neutron) fission processes.

*Acknowledgements.* The authors offer their best wishes to Prof. Poenaru on the occasion of his 70th birthday. The work at Vanderbilt University is supported by U.S. Department of Energy under Grant No. DE-FG05-88ER40407.

## REFERENCES

1. A.V. Ramayya, J.H. Hamilton, J.K. Hwang and G.M. Ter-Akopian, *Heavy elements and related new phenomena*, Volume I, ed. by R.K. Gupta and W. Greiner, World Scientific, Singapore, June 1999, pp. 477–506.
2. G.M. Ter-Akopian *et al.*, Phys. Rev. Lett., **73**, 1477 (1994).
3. G.M. Ter-Akopian *et al.*, Phys. Rev. Lett., **77**, 32 (1996).
4. G.M. Ter-Akopian *et al.*, Phys. Rev., **C 55**, 1146 (1997).
5. S.C. Wu *et al.*, Phys. Rev., **C 62**, 041601 (2000).
6. S.C. Wu *et al.*, Nucl. Instrum. Meth. Phys. Res., **A 480**, 776 (2002).
7. D.C. Radford, Nucl. Instrum. Meth. Phys. Res., **A 361**, 297 (1995).
8. C. Goodin *et al.*, Phys. Rev., **C 74**, 017309 (2006).
9. A. Sandulescu *et al.*, Phys. Rev., **C 54**, 258 (1996).
10. J.H. Hamilton *et al.*, J. Phys., **G 20**, L85 (1994).
11. A. Sandulescu *et al.*, J. Phys. G: Nucl. Part. Phys., **22**, L87 (1996).

12. J.K. Hwang *et al.*, *Nuclei far from stability and astrophysics*, ed. D.N. Poenaru, Kluwer Academic Publishers, Dordrecht, Netherlands, 2001, pp. 173–184.
13. A.C. Wahl, *At. Data Nucl. Data Tables*, **39**, 1 (1988).
14. A. Sandulescu *et al.*, *Int. J. Modern Phys.*, **E 7**, 625 (1998).
15. F.-J. Hamsch, H.-H. Knitter and C. Budtz-Jorgensen, *Nucl. Phys.*, **A 554**, 209 (1993).
16. A.V. Ramayya *et al.*, *Phys. Rev.*, **C 57**, 2370 (1998).
17. A. Sandulescu *et al.*, *Int. Conf. on Fission and Properties of Neutron Rich Nuclei*, Sanibel Island, FL, USA 1997.
18. J.K. Hwang *et al.*, *Phys. Rev.*, **C 61**, 047601 (2000).
19. M. Mutterer, P. Singer, Yu. Kopach, M. Klemens, A. Hotzel, D. Schwalm, P. Thierolf, M. Hesse, in *Proceedings of Dynamical Aspects of Nuclear Fission*, Casta-Papiernicka, Slovak Republic, 1996 Dubna Press, p. 250.
20. I. Halpern, *Ann. Rev. Nucl. Sci.*, **21**, 245 (1971).
21. E. Cheifetz, B. Eylon, E. Fraenkel, A. Gavron, *Phys. Rev. Lett.*, **29**, 805 (1972).
22. C. Wagemans, *The Nuclear Fission Process*, CRC Press, Inc. London, 1991.
23. W. Loveland, *Phys. Rev.*, **C 9**, 395 (1974).
24. Hongyin Han, Shengnian Huang, Jiangchen Meng, Zeongyn Bao, Zougyuan Ye, *IAEA Consults Meet. Physics of Neutron Emission in Fission*, ed. H.D. Lemmel, IAEA, Vienna, 1989.
25. P. D’hondt, A. De Clercq, A. Deruytter, C. Wagemans, M. Asghar and A. Emsallem, *Nucl. Phys.*, **A 303**, 275 (1978).
26. F. Caitucoli, B. Leroux, G. Barreau, N. Carjan, T. Benfoughal, T. Doan, F. El Hage, A. Sicre, M. Asghar, P. Perrin, and G. Siegert, *Z. Phys.*, **A 298**, 219 (1980).
27. A.V. Ramayya *et al.*, *Phys. Rev. Lett.*, **81**, 947 (1998).
28. S. Raman *et al.*, *Atomic Data and Nucl. Data Tables*, **36**, 1 (1987).
29. P. Moller *et al.*, *Atomic Data and Nucl. Data Tables*, **59**, 185 (1995).
30. J.H. Hamilton *et al.*, *Prog. in Part. and Nucl. Phys.*, **35**, 635 (1995).